International Immunopharmacology 133 (2024) 112086

Contents lists available at ScienceDirect

International Immunopharmacology

journal homepage: www.elsevier.com/locate/intimp

The protective effect of Macrostemonoside T from *Allium macrostemon* Bunge against Isoproterenol-Induced myocardial injury via the PI3K/Akt/mTOR signaling pathway

Jianfa Wu [a,1], Ying Cui [a,1], Weixing Ding [a], Jing Zhang [a,*], Lulu Wang [b,*]

[a] Department of Traditional Chinese Medicine, College of Traditional Chinese Medicinal Materials, Jilin Agricultural University, Changchun 130118, China
[b] School of Medicine, Changchun Sci-Tech University, Changchun 130600, China

ARTICLE INFO

Keywords:
Macrostemonoside T
PI3K/Akt/mTOR signaling pathway
Myocardial injury
Cardiovascular disease
Apoptosis

ABSTRACT

Myocardial injury (MI) signifies a pathological aspect of cardiovascular diseases (CVDs) such as coronary artery disease, diabetic cardiomyopathy, and myocarditis. Macrostemonoside T (MST) has been isolated from *Allium macrostemon* Bunge (AMB), a key traditional Chinese medicine (TCM) used for treating chest stuffiness and pains. Although MST has demonstrated considerable antioxidant activity in vitro, its protective effect against MI remains unexplored. To investigate MST's effects in both in vivo and in vitro models of isoproterenol (ISO)-induced MI and elucidate its underlying molecular mechanisms. This study established an ISO-induced MI model in rats and assessed H9c2 cytotoxicity to examine MST's impact on MI. Various assays, including histopathological staining, TUNEL staining, immunohistochemical staining, DCFH-DA staining, JC-1 staining, ELISA technique, and Western blot (WB), were utilized to explore the potential molecular mechanisms of MI protection. In vivo experiments demonstrated that ISO caused myocardial fiber disorders, elevated cardiac enzyme levels, and apoptosis. However, pretreatment with MST significantly mitigated these detrimental changes. In vitro experiments revealed that MST boosted antioxidant enzyme levels and suppressed malondialdehyde (MDA) production in H9c2 cells. Concurrently, MST inhibited ISO-induced reactive oxygen species (ROS) production and mitigated the decline in mitochondrial membrane potential, thereby reducing the apoptosis rate. Moreover, pretreatment with MST elevated the expression levels of p-PI3K, p-Akt, and p-mTOR, indicating activation of the PI3K/Akt/mTOR signaling pathway and consequent protection against MI. MST attenuated ISO-induced MI in rats by impeding apoptosis through activation of the PI3K/Akt/mTOR signaling pathway. This study presents potential avenues for the development of precursor drugs for CVDs.

1. Introduction

Cardiovascular diseases (CVDs) are among the leading causes of human mortality, representing the primary threat to human health [1]. CVDs include conditions such as ischemic heart disease, stroke, heart failure, rheumatic heart disease, and cardiomyopathy [2]. More than 50 % of patients with CVDs are affected by ischemic heart disease, making it the leading cause of death and disability [3,4]. When ischemic heart disease occurs, cardiomyocytes die rapidly due to a variety of factors, including ischemia, hypoxia, and acidosis, which in turn produces severe myocardial injury (MI) [5,6]. As cardiomyocytes are terminally differentiated cells incapable of regeneration, their death due to prolonged ischemia and hypoxia stands as the most lethal factor in CVDs. Preventing cardiomyocyte injury and mortality poses a significant

Abbreviations: MI, myocardial injury; CVDs, cardiovascular diseases; MST, Macrostemonoside T; AMB, *Allium macrostemon* Bunge; TCM, traditional Chinese medicine; ISO, isoproterenol; WB, western blot; MDA, malondialdehyde; ROS, reactive oxygen species; Bcl-2, B-cell lymphoma-2; Bax, Bcl-2-related X protein; SD, Sprague-Dawley; *i.h.*, hypodermic injection; MET, metoprolol; LDH, lactate dehydrogenase; cTn-I, cardiac troponin I; CK-MB, creatine kinase isoenzyme MB; H&E, hematoxylin-eosin; IHC, immunohistochemistry; PBS, phosphate buffer solution; DMEM, Dulbecco's modified Eagle's medium; CCK-8, Cell Counting Kit-8; SOD, superoxide dismutase; CAT, catalase; GSH, reduced glutathione; ΔΨm, mitochondrial membrane potential; BCA, bicinchoninic acid protein assay; TBST, tris buffered saline with tween.

* Corresponding authors.
E-mail addresses: zhangjing4693@jlau.edu.cn (J. Zhang), relulu@126.com (L. Wang).
[1] These authors contributed equally to this work.

https://doi.org/10.1016/j.intimp.2024.112086
Received 27 February 2024; Received in revised form 31 March 2024; Accepted 10 April 2024
Available online 19 April 2024

therapeutic challenge in clinical practice [7]. Therefore, studying the mechanisms of myocardial injury and searching for potential therapeutic agents and targets of action can effectively reduce the loss of cardiac function and improve the prognosis of patients.

Research has demonstrated that myocardial ischemia and hypoxia trigger excessive oxidative stress, resulting in the generation of substantial amounts of reactive oxygen species (ROS). The excessive presence of ROS further prompts apoptosis in cardiomyocytes, impairing cardiac function and contributing to the progression of CVDs [8,9]. The apoptosis process is regulated by the B-cell lymphoma-2 (Bcl-2) family of proteins, where the presence of pro-apoptotic proteins (such as Bcl-2-related X protein, Bax) and the balance of anti-apoptotic proteins (Bcl-2) are crucial indicators in predicting apoptosis [10–12]. When the Bcl-2/Bax ratio is reduced, the cysteine protease-3 cascade is initiated, leading to the cleavage of poly-ADP-ribose polymerase and, ultimately, apoptosis [12,13]. Apoptosis of cardiomyocytes is observed throughout the cardiac remodeling process, persists, and significantly affects the efficacy of antimyocardial ischemic therapy [14]. Therefore, inhibition of cardiomyocyte apoptosis is important for attenuating cardiac dysfunction and is critical for repairing damaged hearts and treating ischemic heart disease [8].

Nowadays, traditional Chinese medicine (TCM) has gained widespread popularity and global usage [15,16]. TCM and its active components find extensive application in both the treatment and prevention of CVDs [17–20]. Among these, *Allium macrostemon* Bunge (AMB) stands prominent, widely recognized in the treatment of "chest stuffiness and pains" [21]. Emerging evidence suggests that the cardioprotective attributes of AMB are due to its steroidal saponins [22–26]. Within this category, Macrostemonoside T (MST) emerges as a novel steroidal saponin isolated from AMB, characterized by the chemical formula spirostane-25(27)-en-2α,3β-diol-3-*O*-β-D-xylopyranosyl(1 → 3)-β-D-glucopyranosyl(1 → 4)-β-D-galactopyranosid (Fig. 1A). While MST has demonstrated significant in vitro antioxidant activity, exhibiting remarkable scavenging capabilities against various free radicals [27], its potential protective role against MI remains to be fully elucidated.

Isoprenaline (ISO) is a β-agonist that acts on β-adrenoceptors on cardiomyocytes to enhance myocardial contraction. Large doses of ISO can increase myocardial oxygen consumption, generate large amounts of ROS, induce cardiac stress, and lead to MI and infarct-like changes, making it a commonly used MI inducer [28–31]. Compared with the coronary artery ligation modeling approach, ISO has the advantages of simpler operation, greater success rate, greater model controllability and greater reduction of discomfort and pain in experimental animals. Therefore, ISO is more suitable for the initial exploration of myocardial injury mechanisms or the evaluation of specific drug treatments.

The PI3K/Akt/mTOR signaling pathway plays a pivotal role in governing apoptosis, proliferation, metabolism, protein synthesis, and inflammation [32,33]. Prior research has highlighted that activation of the PI3K/Akt/mTOR signaling pathway contributes to the mitigation of MI [34–36]. Thus, our current study aims to delineate the involvement of MST in regulating the PI3K/Akt/mTOR signaling pathway amidst ISO-induced MI.

2. Materials and methods

2.1. Animals and treatment

Six weeks old male Sprague-Dawley (SD) rats (190–210 g) were purchased from Changchun, China. They were kept in a standard laboratory environment and were exposed to a 12-hour light cycle. The study followed guidelines set by the NIH for the care and use of laboratory animals. All of the procedures and handling were carried out according to the regulations of the Jilin Agricultural University's Animal Ethics Committee.

After one week, the 36 SD rats were randomly assigned to six groups. ISO (Sigma-Aldrich, MO, USA) was prepared in saline and hypodermically injected (*i.h.*) for two consecutive days at a dosage of 50 mg/kg/day to induce MI. Each group of SD rats was administered the following treatments: control group (Control): the same amount of saline was gavaged for 9 days. Isoprenaline group (ISO): a regular dose of saline was administered by gavage for 7 days, followed by *i.h.* of ISO on days 8 and 9. Groups of MST Low-dose (ISO + MST-L), Medium-dose (ISO + MST-M), and High-dose (ISO + MST-H): from day 1 ~ 7, MST (10, 20, and 40 mg/kg) was administered by gavage every 24 h, followed by *i.h.* of ISO on days 8 and 9. MST was homemade in the laboratory and was ≥ 98.5 % pure. Metoprolol group (MET; AstraZeneca, LON, UK): MET (18 mg/kg) was administered by gavage every 24 h from day 1 ~ 7, followed by *i.h.* of ISO on days 8 and 9 [37].

The rats were anesthetized by *i.h.* of ethyl carbamate 24 h after the last injection of saline and ISO. The thoracic cavity was rapidly opened to allow blood to be collected from the heart and subsequently removed. Portions of the hearts were cryopreserved for later analysis. Additionally, portions of the hearts were immersed in a 4 % paraformaldehyde solution, later undergoing embedding in paraffin for subsequent sectioning and analysis.

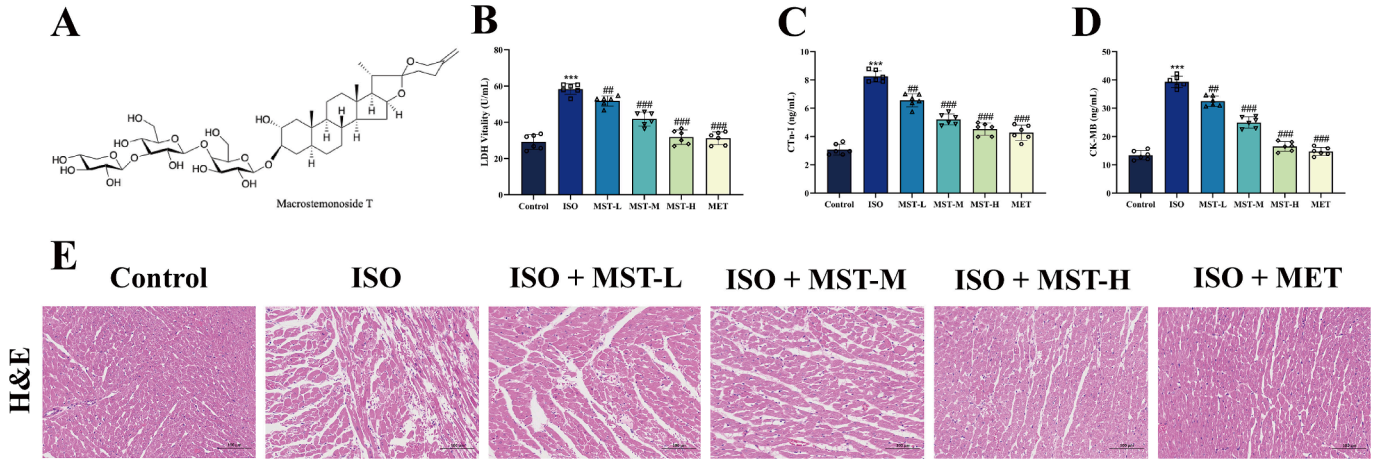

Fig. 1. MST pretreatment ameliorated ISO-induced MI in SD rats. (A) Chemical structure of MST. (B, C, and D) Serum levels of LDH, cTn-I, and CK-MB in SD rats (n = 6). (E) Images of H&E staining (200 ×) of myocardial tissue from SD rats (n = 3). Data are shown as mean ± SD. *** $P < 0.001$ *vs.* control group; $^{\#\#}$ $P < 0.01$, $^{\#\#\#}$ $P < 0.001$ *vs.* ISO group.

2.2. Determination of MI-related enzymes

The serum was obtained by centrifuging the blood at 13,500 r·min^{-1} for 12 min at 4 °C. Subsequently, assays for lactate dehydrogenase (LDH; Solarbio, Beijing, China), cardiac troponin I (cTn-I; Meike, Yancheng, China), and creatine kinase isoenzyme MB (CK-MB; Meike, Yancheng, China) were conducted following the manufacturer's instructions with strict adherence.

2.3. Histopathological studies

Cardiac tissues were sectioned into 4-μm-thick slices after paraffin embedding and stained with a hematoxylin-eosin kit (H&E; Servicebio, Wuhan, China). A light microscope (Nikon Eclipse E100, Tokyo, Japan) was used to observe histological changes in the left ventricle of the heart.

2.4. TUNEL staining

Cardiac tissue sections were subjected to staining using a TUNEL kit (Servicebio, Wuhan, China) to detect myocardial apoptosis, following the precise guidelines provided by the manufacturer. Following staining, the results were observed and documented using an upright fluorescence microscope (Nikon Eclipse C1, Tokyo, Japan). An indicator of myocardial apoptosis was calculated by comparing the percentage of green fluorescent nuclei (TUNEL-positive) with the total number of nuclei stained with DAPI (appearing as blue fluorescent nuclei).

2.5. Immunohistochemistry (IHC)

The paraffin sections underwent dewaxing and rehydration, followed by immersion in 2 % methanol-hydrogen peroxide for 5 min at 27 ℃. Afterward, the sections were washed four times with phosphate buffer solution (PBS). Once the sections had been immersed in citrate buffer (0.01 M, pH 6.2) and microwaved for 12 min, they were cooled to 27 °C and washed four times with PBS. Following this, the tissue sections were blocked using goat serum (Bosterbio, Wuhan, China) for 30 min at 27 ℃. A primary antibody against Bax (1:150) and Bcl-2 (1:100) (Bosterbio, Wuhan, China) was then incubated overnight at 4 °C with the sections. Following incubation, the sections of tissue were washed four times with PBS before being treated with secondary antibodies (Zsgbbio, Beijing, China) and incubated at 37 °C for 45 min. A BX51T-PHD-J11 microscope (Olympus Co., Ltd., Tokyo, Japan) was used for staining observations, and ImageJ was used for analysis.

2.6. H9C2 cardiomyocyte culture and therapy

H9c2 cells were procured from the American Type Culture Collection. These cells were cultured in DMEM (Gibco, NY, USA) supplemented with 10 % FBS (Gibco, NY, USA) and 1 % penicillin–streptomycin (Genview, Changsha, China). In an incubator with 5 % CO_2, the cells were maintained at 37 °C. A three-day cycle of medium replenishment was followed. Cells were divided into control, ISO, and administration groups. The ISO group received treatment with ISO (200 μM) for 12 h, except for the control group. In the administration group, cells were pretreated with the corresponding concentration of MST (1 μM, 2 μM, or 5 μM) for 24 h before ISO treatment.

2.7. Cell viability assays

The H9c2 cells were assessed for viability using Cell Counting Kit-8 (CCK-8; Biosharp, Beijing, China). The H9c2 cells were inoculated into 96-well plates at a ratio of 5×10^3 cells per well, and they were cultured for 24 h thereafter. After cell administration, 10 μL of CCK-8 was added to each well and incubated for 2 h, protected from light. The absorbance value at 450 nm was measured in each well using the SPECTRO star Nano full-wavelength enzyme labeler (BMG LABTECH, Offenburg, Germany), and the cell viability was calculated based on these measurements.

2.8. Determination of LDH, superoxide dismutase (SOD), catalase (CAT), reduced glutathione (GSH) and malondialdehyde (MDA) content

H9c2 cells were inoculated in 6-well plates at a ratio of 5×10^5 cells per well, and the cells were cultured for 24 h thereafter. Upon reaching 24 h of culture, the supernatant was collected, and assays for LDH, SOD, CAT, GSH, and MDA were performed following the instructions provided with the assay kit (Solarbio, Beijing, China).

2.9. ROS and mitochondrial membrane potential (ΔΨm) detection

We measured ROS levels in H9c2 cells using the ROS detection kit (Solarbio, Beijing, China). In a 37 °C cell culture incubator, cells from each group were stained with DCFH-DA for 18 min. The cells were washed four times in PBS following incubation. An inverted fluorescence microscope was used to observe and document the stained cells (Leica TCS SP8, Solms, Germany).

Assessing the ΔΨm of H9c2 cells was done quantitatively through the JC-1 assay kit (Solarbio, Beijing, China). In a 37 °C cell culture incubator, cells from each group were stained with JC-1 staining working solution for 13 min. Afterwards, the cells were washed three times with JC-1 staining buffer that had been pre-cooled. The staining results were recorded under an inverted fluorescence microscope (Leica TCS SP8, Solms, Germany) after adding 2 mL of cell culture solution to each well.

2.10. Hoechst 33258 staining

Hoechst 33258 (Solarbio, Beijing, China) is a DNA-stainable nuclear staining reagent for apoptosis detection. In each group, cells were fixed in methanol for 13 min, followed by four washes with PBS. We incubated the cells in each group in an incubator protected from light for 8 min at 37 °C to stain them with Hoechst 33258 staining solution (10 μM in PBS). Using an inverted fluorescence microscope (Leica TCS SP8, Solms, Germany), apoptotic nuclei with blue fluorescence were observed and recorded.

2.11. Western blot (WB) analysis

RIPA lysis buffer (NCM Biotech, Suzhou, China) was used to extract total proteins from cardiac tissues or cells. A bicinchoninic acid protein assay kit (BCA; Beyotime, Shanghai, China) was used to determine the protein concentration. It was determined that equal quantities of proteins were loaded onto an 8 % or 12 % SDS-PAGE gel, and then transferred to a PVDF membrane (Millipore, Darmstadt, Germany). After that, the PVDF membranes were blocked in 5 % skimmed milk containing tris buffered saline with tween (TBST; Servicebio, Wuhan, China) at 27 °C for 1.5 h. As soon as the membranes had been blocked, they were washed with TBST buffer and incubated overnight with the corresponding primary antibodies at 4 °C. Dilute primary antibodies using TBST to the following ratios, respectively: PI3K (1:1500), p-PI3K (1:1500), Akt (1:800), p-Akt (1:800), mTOR (1:1500), p-mTOR (1:500), Bcl-2 (1:800), Bax (1:800), and GAPDH (1:800) (Wanleibio, Shenyang, China). The membranes were washed with TBST after primary antibody incubation and subsequently incubated for 1.5 h at 27 °C with secondary antibodies labeled with horseradish peroxidase (Biodragon, Suzhou, China). Tanon 5200 chemiluminescent imaging system (Tanon Science and Technology Co., Ltd., Shanghai, China) was used to visualize and measure protein levels, and ImageJ software was utilized for analysis.

2.12. Statistical analysis

A mean and standard error were calculated for all data. A one-way analysis of variance was conducted using GraphPad Prism software to

assess the differences between the groups. Graphs were generated based on the obtained statistical outcomes. Statistical significance was defined as $P < 0.05$.

3. Results

3.1. MST reduces ISO-induced MI

The serum levels of LDH, cTn-I, and CK-MB were examined to determine whether MST protected rats from ISO-induced MI. It can be seen from Fig. 1B–D that LDH, cTn-I, and CK-MB levels in the serum of rats in the ISO group were significantly higher than those in the control group ($P < 0.001$), suggesting that ISO is capable of causing MI in rats. In each administered group, treatment significantly decreased LDH, cTn-I, and CK-MB serum levels in a dose-dependent manner compared to the ISO group ($P < 0.01$ or $P < 0.001$). Levels in the MST-H group closely resembled those in the MET group.

H&E staining was used to detect the histopathological changes of MI in rats. It was observed in Fig. 1E that the myocardium was neatly arranged and tightly packed, with clear striations, and that there were no obvious changes in the myocardial morphology of the control group. However, severe damage was observed in the myocardial tissues of rats in the ISO group, as evidenced by the disarranged and fractured myocardial fibers, enlarged gaps in myocardial fibers, necrosis, interstitial remodeling, and a large number of inflammatory cells infiltration. In contrast, MST-L and MST-M preconditioning were able to ameliorate such changes. MET and MST-H preconditioning were able to normalize such changes, demonstrating that MST preconditioning was effective in ameliorating ISO-induced MI.

3.2. MST reduces ISO-induced apoptosis in rat myocardium

An assessment of the level of apoptosis in rat cardiomyocytes is performed using TUNEL staining. In this process, the nuclei of healthy cardiomyocytes exhibit blue fluorescence, while the nuclei of apoptotic cells demonstrate green fluorescence (indicating positive cells). It is evident from Fig. 2A that the control group showed minimal positive cells, whereas the ISO group displayed a number of TUNEL-positive cells ($P < 0.001$). In Fig. 2B, rats injected with ISO exhibited a TUNEL-positive rate of cardiomyocytes at 13.38 %, significantly higher than the 0.55 % in the control group. However, in rats pretreated with MST, there was a dose-dependent decrease in the TUNEL-positive rate of cardiomyocytes. Specifically, the rates in the MST-L, MST-M, and MST-H groups reached 11.75 %, 9.41 %, and 0.63 %, respectively. The positivity rate of the MET group was 0.57 %. The results indicated that MST could reduce ISO-induced apoptosis in rat cardiomyocytes.

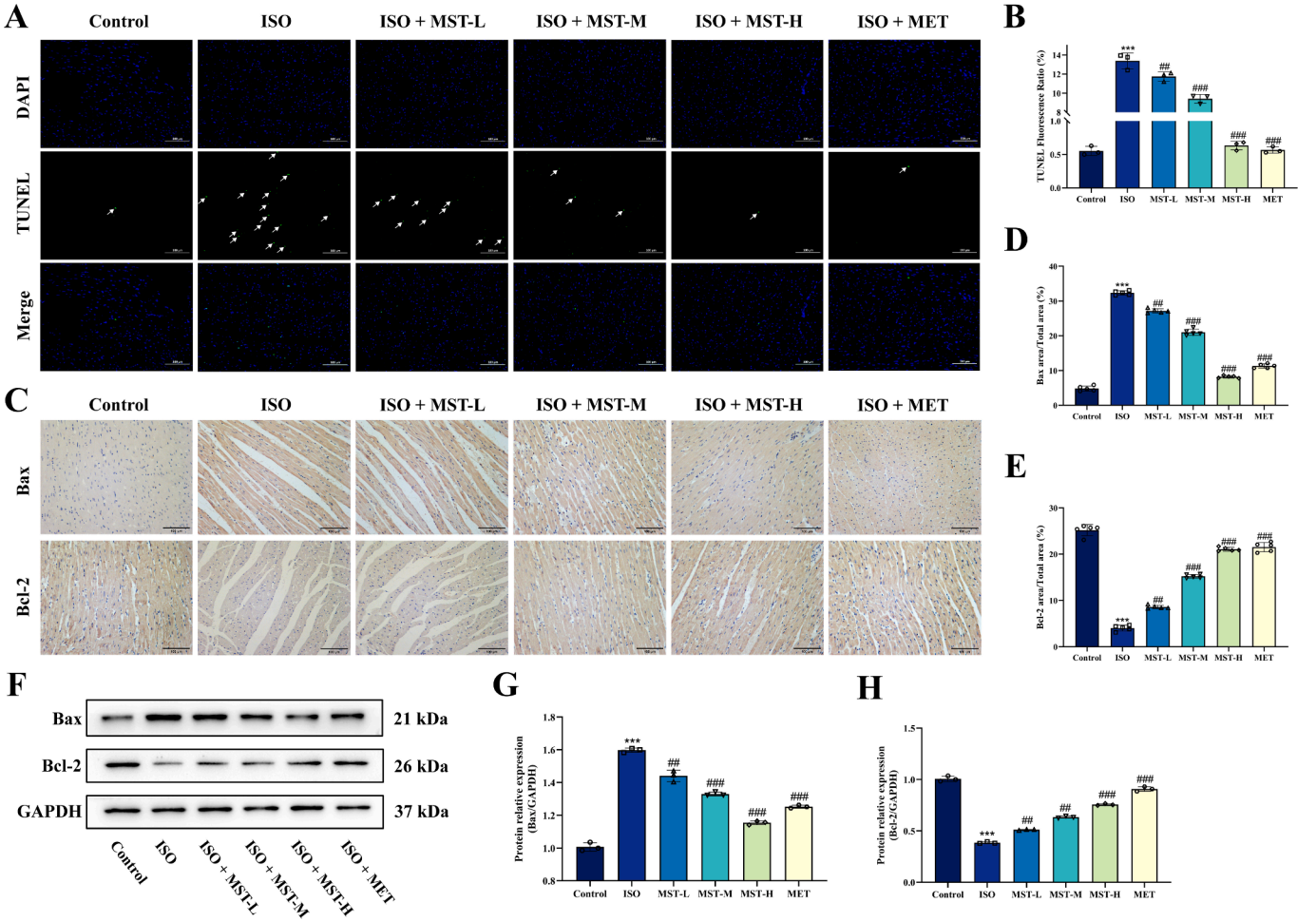

Fig. 2. MST pretreatment reduced ISO-induced myocardial apoptosis in SD rats. (A) TUNEL-stained images ($n = 3$) of SD rat left ventricular cardiomyocytes, (200×, nuclei of normal cells showed blue fluorescence, nuclei of TUNEL apoptotic cells showed green fluorescence). (B) TUNEL apoptosis rate analysis ($n = 3$). (C) Images of IHC staining to detect Bax and Bcl-2 expression in SD rat myocardial tissues ($n = 5$), (200×, brown particles for protein expression). (D and E) Analysis of Bax and Bcl-2 expression levels in SD rat myocardial tissues ($n = 5$). (F) WB analysis of Bax, Bcl-2, and GAPDH proteins in SD rat myocardial tissues ($n = 3$). (G and H) Quantitative analysis of the ratio of Bax and Bcl-2 to GAPDH in protein expression in SD rat myocardial tissue, respectively ($n = 3$). Data are shown as mean ± SD. *** $P < 0.001$ *vs.* control group; $^{\#\#}$ $P < 0.01$, $^{\#\#\#}$ $P < 0.001$ *vs.* ISO group.

A comparison of ISO and control groups by IHC showed (Fig. 2C–E) that Bax protein expression significantly increased in the ISO group and that Bcl-2 protein expression significantly decreased ($P < 0.001$), further demonstrating that ISO causes cardiomyocyte apoptosis. Notably, MET and different doses of MST reversed the above changes ($P < 0.01$ or $P < 0.001$). Furthermore, WB was used to examine the expression levels of Bax and Bcl-2 proteins in rat myocardium. According to Fig. 2F–H, similarly to the results of IHC, the expression level of the apoptotic protein Bax was significantly increased, while the expression level of the anti-apoptotic protein Bcl-2 was significantly decreased in the ISO group compared with the control group ($P < 0.001$). Compared with the ISO group, however, the expression level of Bax was significantly reduced and the expression level of Bcl-2 was significantly increased in groups pretreated with MET and different doses of MST ($P < 0.01$ or $P < 0.001$). As a result of these findings, MST was found to be effective in reducing ISO-induced myocardial apoptosis in rats.

3.3. Protective effect of MST against ISO-induced H9c2 cell injury

MST was found to protect H9c2 cells from ISO-induced cell damage via the CCK-8 assay, and different concentrations of MST and ISO were examined for their effects on cell viability. In the dose range of 0.5–20 μM, MST exhibited no significant cytotoxicity to cells and displayed some proliferative activity compared to the control group (Fig. 3A, $P < 0.05$ or $P < 0.001$). Therefore, 1, 2 and 5 μM were chosen as the concentrations for MST pretreatment in the subsequent experiments. As shown in Fig. 3B, there was a notable decrease in the viability of H9c2 cells correlating with increased ISO concentration ($P < 0.05$ or $P < 0.001$). Overall, ISO induced damage to the cells, and at a 200 μM concentration for 12 h, cell viability decreased to around 60 %. Hence, the utilization of a 200 μM ISO treatment for 12 h served as the benchmark for inducing damage in cells.

In an attempt to study how MST affects ISO-induced cell damage in H9c2 cells, H9c2 cells were pretreated with 1, 2, and 5 μM MST for 24 h, followed by 12 h incubation in DMEM medium containing ISO at a concentration of 200 μM. In Fig. 3C, the outcomes of the CCK-8 assay revealed a notable decrease in cell viability within the ISO group compared to the control group ($P < 0.001$). Pretreatment with varying doses of MST notably increased the viability of H9c2 cells in a dose-dependent fashion compared to the ISO group ($P < 0.01$ or $P < 0.001$). Furthermore, LDH served as the primary indicator for evaluating cell membrane damage (Fig. 3D). Upon exposure to ISO, the cell membrane experienced rupture, leading to a notable increase in LDH levels ($P < 0.001$). Conversely, the cell membrane integrity was safeguarded following pretreatment with various concentrations of MST, leading to a significant reduction in LDH release and consequently enhancing cell survival ($P < 0.05$ or $P < 0.01$). According to the above results, MST significantly reduced the damage caused by ISO to H9c2 cells.

3.4. MST increased the activity of antioxidant enzymes in H9c2 cells and inhibited the production of MDA and ROS therein

To determine if the protective effect of MST against ISO-induced damage is related to the reduction of oxidative stress, antioxidant enzymes (SOD and CAT) were tested and GSH and MDA levels were assessed in H9c2 cells. In comparison with the control group, treatment with ISO significantly reduced antioxidant enzyme levels and GSH levels ($P < 0.001$), whereas it significantly increased MDA levels ($P < 0.001$) (Fig. 4A–D). In comparison to the ISO group, pretreatment with MST increased antioxidant enzyme activities and GSH levels ($P < 0.05$, $P <$

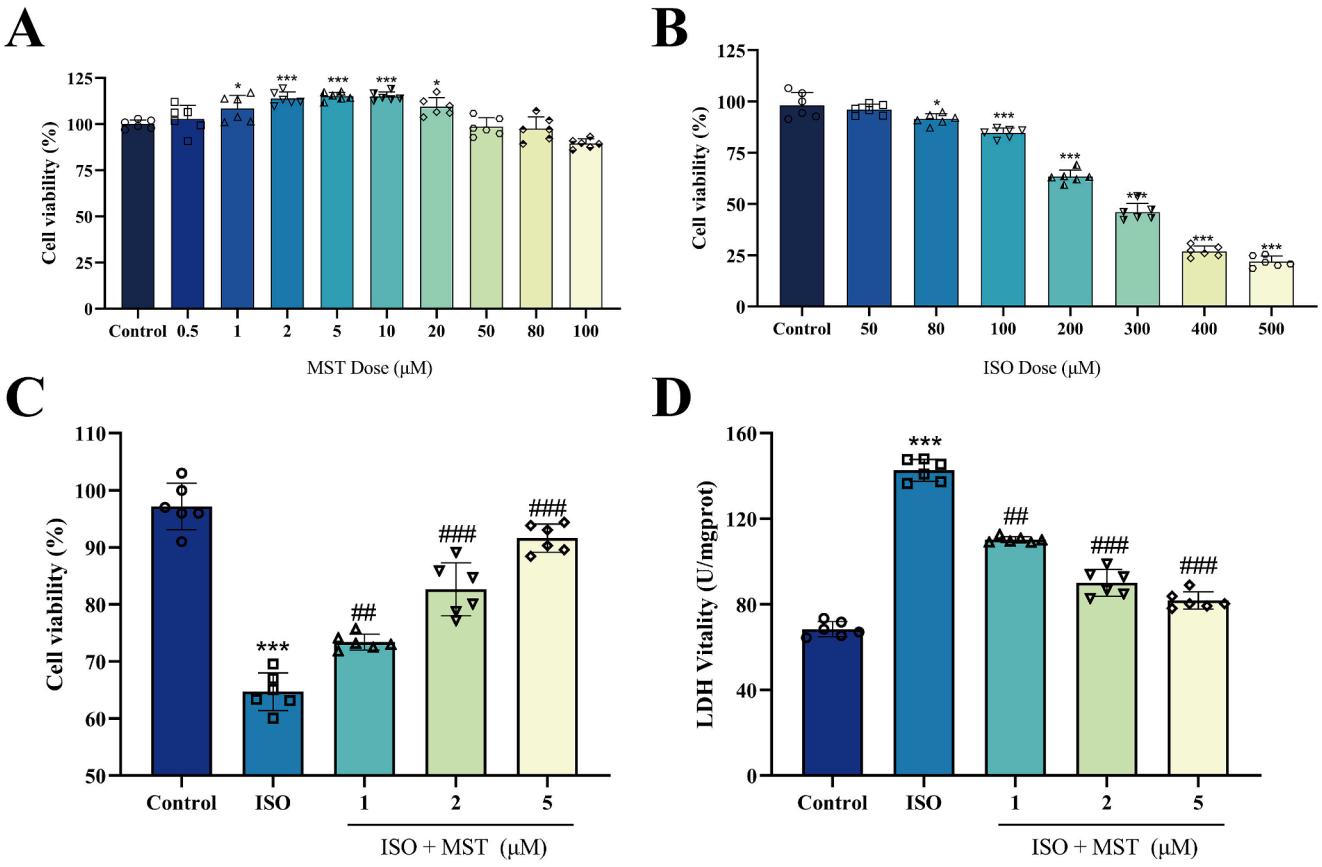

Fig. 3. MST pretreatment is protective against ISO-induced H9c2 cell damage. (A) Effect of MST on H9c2 cell viability ($n = 6$). (B) Effect of ISO on H9c2 cell viability ($n = 6$). (C) Effect of MST on the viability of ISO-treated H9c2 cells ($n = 6$). (D) Effect of MST on LDH release from ISO-treated H9c2 cells ($n = 6$). Data are shown as mean ± SD. * $P < 0.05$, *** $P < 0.001$ *vs.* control group; ## $P < 0.01$, ### $P < 0.001$ *vs.* ISO group.

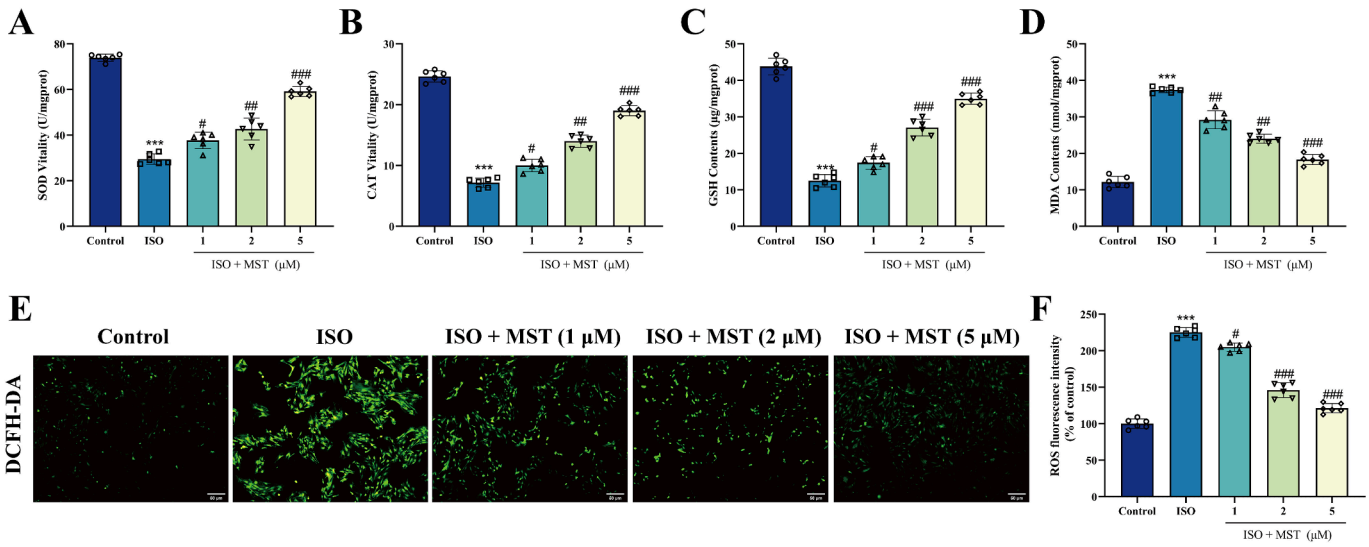

Fig. 4. MST pretreatment increases the activity of antioxidant enzymes and inhibits the production of MDA and ROS in H9c2 cells. (A and B) Activity analysis of SOD and CAT in H9c2 cells ($n = 6$). (C and D) Expression levels of GSH and MDA were analyzed in H9c2 cells ($n = 6$). (E) Images of DCFH-DA staining to detect ROS levels in H9c2 cells ($n = 6$), (400×, green fluorescence represents ROS staining). (F) Quantitative analysis of ROS levels in H9c2 cells ($n = 6$). Data are shown as mean ± SD. *** $P < 0.001$ *vs.* control group; $^{\#}$ $P < 0.05$, $^{\#\#}$ $P < 0.01$, $^{\#\#\#}$ $P < 0.001$ *vs.* ISO group.

0.01 or $P < 0.001$) and effectively inhibited the production of MDA in the cells ($P < 0.01$ or $P < 0.001$). Consequently, MST increases antioxidant enzyme activity, which results in antagonizing ISO-induced damage to H9c2 cells.

Notably, MDA is a product of lipid peroxidation, and ROS is one of the conditions that cause lipid peroxidation. Therefore, we examined the effect of MST pretreatment on ROS in H9c2 cells. The results are shown in Fig. 4E and F. After treatment with ISO, the fluorescence intensity of ROS in H9c2 cells significantly increased compared to the control group ($P < 0.001$). Under the precondition of MST pretreatment, it could be visually observed that MST effectively inhibited ISO-induced ROS generation in H9c2 cells ($P < 0.05$ or $P < 0.001$). By reducing ROS generation, these results suggest that MST may be able to protect H9c2 cells against ISO-induced oxidative damage.

3.5. MST inhibits ISO-induced apoptosis in H9c2 cells

A small amount of Hoechst 33258 dye can enter normal cells, giving them a light blue hue. When apoptosis occurs and chromatin aggregates, the dye enters the cells in large quantities and gives the nuclei a bright blue color as a result of the increased permeability of the cell membrane. The results of the Hoechst 33,258 staining (Fig. 5A and B) showed that there were few bright blue nuclei in the control group but a large number of bright blue nuclei were observed in the ISO group ($P < 0.001$), indicating the presence of a large number of apoptotic cells in the ISO group. A significant reduction in bright blue nuclei was observed in the groups pretreated with different doses of MST ($P < 0.01$ or $P < 0.001$), suggesting that MST inhibits ISO-induced apoptosis in H9c2 cells.

Furthermore, WB analysis (Fig. 5C–E) demonstrated that ISO treatment significantly increased Bax protein expression in H9c2 cells and decreased Bcl-2 protein expression ($P < 0.001$). Compared with the ISO group, MST pretreatment significantly reversed the expression levels of both proteins ($P < 0.05$, $P < 0.01$, or $P < 0.001$). It was further demonstrated that MST treatment could prevent ISO-induced apoptosis in H9c2 cells.

A decrease in ΔΨm is considered to be the earliest event that occurs during the apoptotic cascade. JC-1 was used to assess the effect of MST on ΔΨm in H9c2 cells. Treatment with ISO significantly reduced the ratio of red/green fluorescence in mitochondria compared to control ($P < 0.001$), indicating depolarization of mitochondria. Pretreatment with 1, 2, and 5 μM of MST exerted varying degrees of protective effects against ISO-induced decrease in ΔΨm in H9c2 cells (Fig. 5F and G, $P < 0.05$, $P < 0.01$, or $P < 0.001$).

3.6. MST activates the PI3K/Akt/mTOR signaling pathway in vivo and in vitro

To further investigate the relationship between the anti-apoptotic effects of MST on the PI3K/Akt/mTOR signaling pathway, we examined the kinetics involved in the control of PI3K, Akt, and mTOR activation both in vivo and in vitro. Based on WB results (Fig. 6A–H), we found that compared with the control group, p-PI3K, p-Akt, and p-mTOR expression levels in the ISO group were significantly lower ($P < 0.001$). Whereas different doses of MST treatment restored the phosphorylation levels of PI3K, Akt, and mTOR in vivo and in vitro to varying degrees, 1 μM of MST did not statistically alter the expression levels of p-Akt in H9c2 cells ($P > 0.05$). The above results suggest that MST inhibits ISO-induced MI and apoptosis of H9c2 cells in rats by activating the PI3K/Akt/mTOR signaling pathway.

4. Discussion

With the increase of social pressure, the incidence of CVDs has been increasing year by year, seriously jeopardizing human health [38]. AMB finds extensive utilization in CVDs treatments [39]. MST is a novel steroidal saponin found in AMB, and MST has been shown to have strong antioxidant activity, which gives it the ability to scavenge ROS [27]. However, MST's cardioprotective role and molecular mechanisms are not clear. In this study, we elucidated the protective influence of MST against ISO-induced MI, primarily attributed to MST's activation of the PI3K/Akt/mTOR signaling pathway.

ISO, a β-agonist, primarily serves clinically to treat bradycardia. However, excessive doses of ISO can produce a considerable volume of ROS through auto-oxidation. This results in myocardial ischemia, hypoxia, and potentially necrosis of cardiomyocytes [28,29]. In this study, we employed subcutaneous injection of ISO to create a MI model in SD rats. MET, a clinical drug for treating myocardial infarction, served as the positive control [37]. Assessing serum myocardial enzyme activity is crucial in determining the severity of MI. Typically, myocardial enzymes

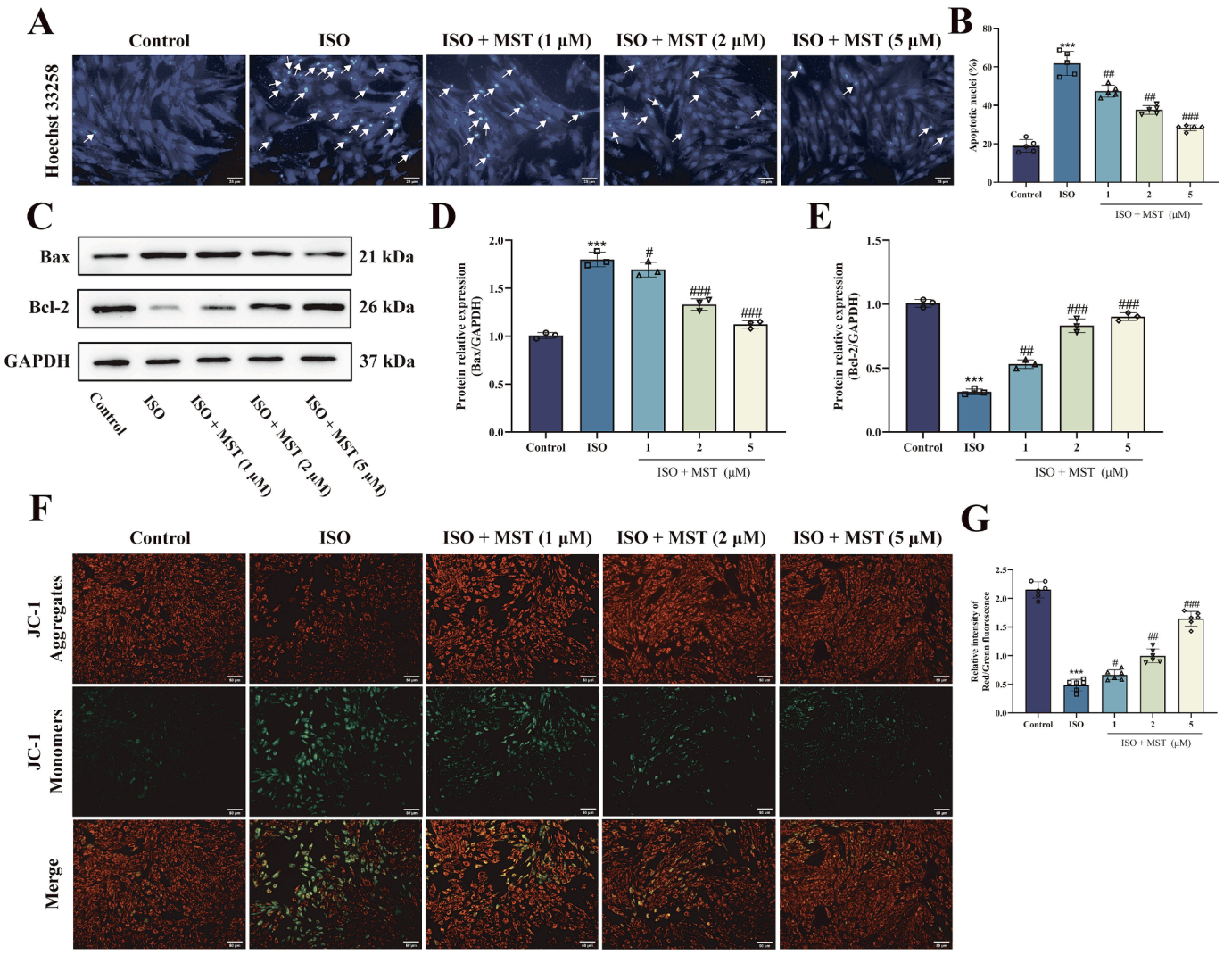

Fig. 5. MST pretreatment alleviates ISO-induced apoptosis in H9c2 cells. (A) Images of Hoechst 33,258 staining for detection of apoptosis ($n = 5$), (800×, bright blue fluorescence represents apoptotic cell nuclei). (B) Hoechst 33,258 staining of H9c2 cells for apoptosis rate analysis ($n = 5$). (C) WB analysis of Bax, Bcl-2, and GAPDH proteins in H9c2 cells ($n = 3$). (D and E) Quantitative analysis of the ratio of Bax and Bcl-2 to GAPDH in protein expression of H9c2 cells, respectively ($n = 3$). (F) Images of JC-1 staining for detection of mitochondrial membrane potential ($n = 3$) in H9c2 cells, (400×, red fluorescence represents normal mitochondria, green fluorescence represents membrane depolarized mitochondria). (G) Quantitative analysis of red/green light in JC-1 staining ($n = 3$). Data are shown as mean ± SD. *** $P < 0.001$ *vs.* control group; $^{\#}$ $P < 0.05$, $^{\#\#}$ $P < 0.01$, $^{\#\#\#}$ $P < 0.001$ *vs.* ISO group.

reside within the cardiomyocyte cytoplasm under normal conditions, and extracellular levels of these enzymes remain exceedingly low. However, when myocardial cells undergo injury, cell rupture causes a substantial release of myocardial enzymes into circulation, elevating serum levels [40,41]. In vivo experiments demonstrated that various doses of MST significantly inhibited LDH, cTn-I, and CK-MB activities in ISO-induced MI in rats. Histopathological findings indicated that MST effectively mitigated ISO-induced myocardial fiber disorganization, enlargement of fiber gaps, and infiltration of inflammatory cells in rats.

Apoptosis is an important link between MI and myocardial remodeling, and improving apoptosis can play a beneficial role in cardiac function. Studies have shown that Bcl-2 inhibits endogenous apoptosis in the myocardium by forming a heterodimer with the pro-apoptotic protein Bax and inhibiting its activity, which further protects myocardial function [42,43]. In our study, both in vivo and in vitro experiments revealed that MST suppressed the expression of Bax and enhanced the expression of Bcl-2 in rat myocardial tissues or H9c2 cells. At the same time, the results of TUNEL, IHC, and Hoechst 33,258 staining also corroborated that MST could effectively inhibit ISO-induced apoptosis in rat cardiomyocytes or apoptosis in H9c2 cells. Oxidative stress is found when the homeostasis of ROS and antioxidant systems in organisms is disrupted. This leads to a high production of ROS, which mediates the production of MDA from membrane lipid peroxidation and further impairs the activity of antioxidant enzymes [44–46]. The data from the present study show that MST reduces the ROS burst and the production of MDA in H9c2 cells as a result of ISO treatment and increases the activity of SOD and CAT as well as the level of GSH. Increased ROS in mitochondria leads to mitochondrial damage, resulting in elevated mitochondrial membrane permeability and decreased ΔΨm, which in turn triggers apoptosis [47,48]. Unsurprisingly, JC-1 staining showed that MST effectively ameliorated ISO-induced decrease in ΔΨm in H9c2 cells. These results suggest that MST may prevent MI through anti-apoptosis and reduction of oxidative stress.

Activation of the PI3K/Akt/mTOR signaling pathway has been reported to reduce apoptosis and regulate myocardial energy metabolism, thereby affecting cardiac function [49,50]. Akt, as a key component of the PI3K/Akt/mTOR signaling pathway, can be phosphorylated by PI3K-produced phosphatidylinositol-3,4,5-trisphosphate, resulting in activation [51]. mTOR, which functions as a downstream target protein of Akt, undergoes activation when Akt phosphorylates it at the Ser2448

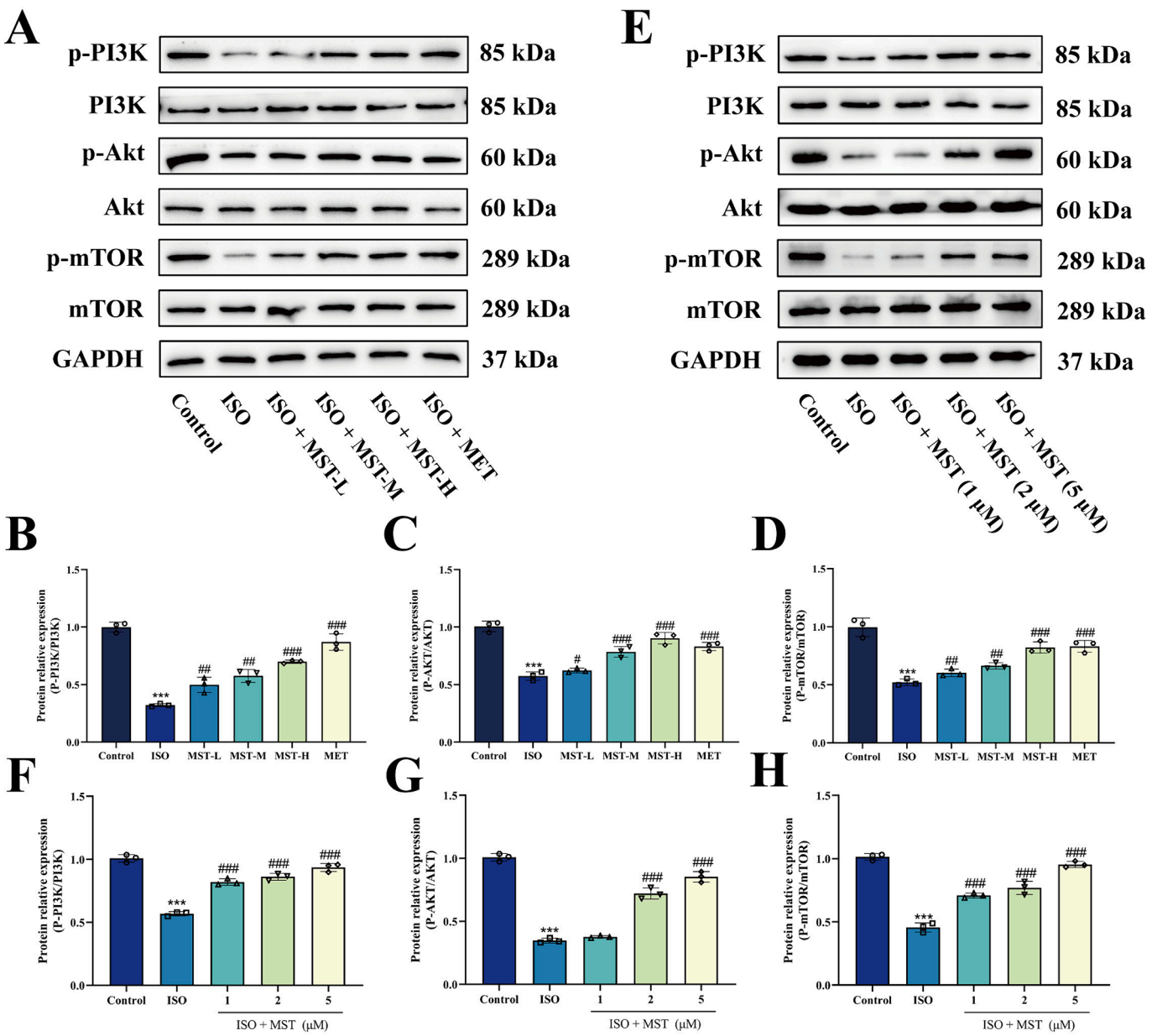

Fig. 6. Expression of PI3K/Akt/mTOR signaling pathway-related proteins in left ventricular myocardial tissues and H9c2 cells of SD rats. (A) WB analysis of PI3K, p-PI3K, Akt, p-Akt, mTOR, p-mTOR, and GAPDH proteins in left ventricular myocardial tissues of SD rats ($n = 3$). (B-D) Quantitative analysis of the ratios of p-PI3K/PI3K, p-Akt/Akt, and p-mTOR/mTOR in protein expression in left ventricular myocardial tissues of SD rats ($n = 3$). (E) WB analysis of PI3K, p-PI3K, Akt, p-Akt, mTOR, p-mTOR, and GAPDH proteins in H9c2 cells ($n = 3$). (F-H) Quantitative analysis of the ratio of p-PI3K/PI3K, p-Akt/Akt, and p-mTOR/mTOR in protein expression in H9c2 cells ($n = 3$). Data are shown as mean ± SD. *** $P < 0.001$ *vs.* control group; $^{\#}$ $P < 0.05$, $^{\#\#}$ $P < 0.01$, $^{\#\#\#}$ $P < 0.001$ *vs.* ISO group.

site. Alternatively, Akt can indirectly activate mTOR by inhibiting tuberous sclerosis complexes 1 and 2. Activation of mTOR, in turn, regulates various physiological functions such as cell proliferation, apoptosis, and migration [52,53]. Several Chinese herbal formulas or activators have shown the ability to alleviate CVDs by activating the PI3K/Akt/mTOR signaling pathway, thereby mitigating MI [34,54,55]. In our study, MST increased the expression levels of p-PI3K, p-Akt and p-mTOR compared to the ISO group. This discovery potentially elucidates the mechanism behind MST's protective impact against ISO-induced MI. Additionally, it suggests a beneficial role in preventing cardiovascular system damage and repairing damaged myocardial tissue.

It should not be overlooked that both autophagy and oxidative stress are closely related to CVDs [56–60]. Shortly, we will carry out in-depth studies on MST against MI in autophagy- and oxidative stress-related signaling pathways accordingly.

5. Conclusion

In conclusion, this study demonstrated the ability of MST, a novel steroidal saponin from AMB, to counteract ISO-induced MI by inhibiting cardiac enzyme levels, increasing antioxidant enzyme levels, inhibiting apoptosis, and activating the PI3K/Akt/mTOR signaling pathway (Fig. 7). Thus, these findings provide new therapeutic strategies and pathways for the treatment of cardiovascular diseases and the development of precursor drugs. In addition, these findings provide new perspectives to study the pharmacological mechanisms of steroidal saponins in AMB.

CRediT authorship contribution statement

Jianfa Wu: Writing – original draft, Validation, Investigation. **Ying**

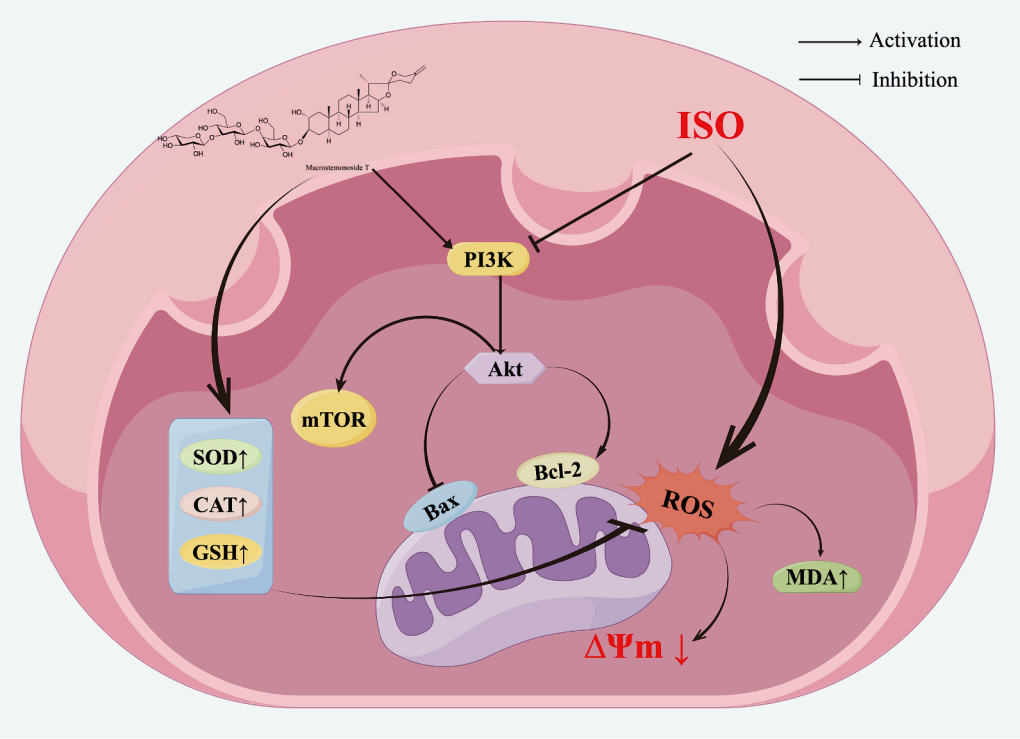

Fig. 7. Schematic representation of MST inhibition of ISO-induced MI through activation of the PI3K/Akt/mTOR signaling pathway (By Figdraw). Treatment with ISO elevates ROS levels in cardiomyocytes and mitochondria, increases MDA production, and decreases ΔΨm. Pretreatment with MST reverses these adverse changes by activating the PI3K/Akt/mTOR signaling pathway and increasing antioxidant enzyme activity.

Cui: Writing – original draft, Validation, Investigation. **Weixing Ding:** Investigation, Formal analysis. **Jing Zhang:** Writing – review & editing, Supervision, Funding acquisition, Conceptualization. **Lulu Wang:** Writing – review & editing, Supervision.

Declaration of Competing Interest

The authors declare that they have no known competing financial interests or personal relationships that could have appeared to influence the work reported in this paper.

Data availability

The data that has been used is confidential.

Acknowledgements

This work was funded by the National Key Research and Development Program of China (2019YFE0116800), and the Jilin Science and Technology Development Program Project (20240305012YY). I would like to thank my lover, Ms. Ying Cui, for her hard work and help in this experiment.

References

[1] E.J. Benjamin, P. Muntner, A. Alonso, M.S. Bittencourt, C.W. Callaway, A. P. Carson, A.M. Chamberlain, A.R. Chang, S. Cheng, S.R. Das, F.N. Delling, L. Djousse, M.S.V. Elkind, J.F. Ferguson, M. Fornage, L.C. Jordan, S.S. Khan, B. M. Kissela, K.L. Knutson, T.W. Kwan, D.T. Lackland, T.T. Lewis, J.H. Lichtman, C. T. Longenecker, M.S. Loop, P.L. Lutsey, S.S. Martin, K. Matsushita, A.E. Moran, M. E. Mussolino, M. O'Flaherty, A. Pandey, A.M. Perak, W.D. Rosamond, G.A. Roth, U. K.A. Sampson, G.M. Satou, E.B. Schroeder, S.H. Shah, N.L. Spartano, A. Stokes, D. L. Tirschwell, C.W. Tsao, M.P. Turakhia, L.B. VanWagner, J.T. Wilkins, S.S. Wong, S.S. Virani, Heart Disease and Stroke Statistics-2019 Update: A Report From the American Heart Association, Circulation 139 (2019) e56–e528, https://doi.org/10.1161/CIR.0000000000000659.

[2] G.A. Mensah, G.A. Roth, V. Fuster, The Global Burden of Cardiovascular Diseases and Risk Factors: 2020 and Beyond, J. Am. Coll. Cardiol. 74 (2019) 2529–2532, https://doi.org/10.1016/j.jacc.2019.10.009.

[3] G.A. Roth, G.A. Mensah, C.O. Johnson, G. Addolorato, E. Ammirati, L.M. Baddour, N.C. Barengo, A.Z. Beaton, E.J. Benjamin, C.P. Benziger, A. Bonny, M. Brauer, M. Brodmann, T.J. Cahill, J. Carapetis, A.L. Catapano, S.S. Chugh, L.T. Cooper, J. Coresh, M. Criqui, N. DeCleene, K.A. Eagle, S. Emmons-Bell, V.L. Feigin, J. Fernández-Solà, G. Fowkes, E. Gakidou, S.M. Grundy, F.J. He, G. Howard, F. Hu, L. Inker, G. Karthikeyan, N. Kassebaum, W. Koroshetz, C. Lavie, D. Lloyd-Jones, H. S. Lu, A. Mirijello, A.M. Temesgen, A. Mokdad, A.E. Moran, P. Muntner, J. Narula, B. Neal, M. Ntsekhe, G. Moraes de Oliveira, C. Otto, M. Owolabi, M. Pratt, S. Rajagopalan, M. Reitsma, A.L.P. Ribeiro, N. Rigotti, A. Rodgers, C. Sable, S. Shakil, K. Sliwa-Hahnle, B. Stark, J. Sundström, P. Timpel, I.M. Tleyjeh, M. Valgimigli, T. Vos, P.K. Whelton, M. Yacoub, L. Zuhlke, C. Murray, V. Fuster, Global Burden of Cardiovascular Diseases and Risk Factors, 1990–2019: Update From the GBD 2019 Study, J. Am. Coll. Cardiol. 76 (2020) 2982–3021, https://doi.org/10.1016/j.jacc.2020.11.010.

[4] K. Thygesen, J.S. Alpert, A.S. Jaffe, B.R. Chaitman, J.J. Bax, D.A. Morrow, H. D. White, Fourth Universal Definition of Myocardial Infarction (2018), Circulation 138 (2018) e618–e651, https://doi.org/10.1161/CIR.0000000000000617.

[5] S. Sanada, I. Komuro, M. Kitakaze, Pathophysiology of myocardial reperfusion injury: preconditioning, postconditioning, and translational aspects of protective measures, Am. J. Physiol. Heart Circ. Physiol. 301 (2011) 1723–1741, https://doi.org/10.1152/ajpheart.00553.2011.

[6] M. Tibaut, D. Mekis, D. Petrovic, Pathophysiology of myocardial infarction and acute management strategies, Cardiovasc. Hematol. Agents Med. Chem. 14 (2016) 150–159, https://doi.org/10.2174/1871525714666161216100553.

[7] Y. Wu, Y. Wang, X. Nabi, Protective effect of Ziziphora clinopodioides flavonoids against H(2)O(2)-induced oxidative stress in HUVEC cells, Biomed. Pharmacother. 117 (2019) 109156, https://doi.org/10.1016/j.biopha.2019.109156.

[8] Y.J. Wei, J.F. Wang, F. Cheng, H.J. Xu, J.J. Chen, J. Xiong, J. Wang, miR-124-3p targeted SIRT1 to regulate cell apoptosis, inflammatory response, and oxidative stress in acute myocardial infarction in rats via modulation of the FGF21/CREB/PGC1α pathway, J. Physiol. Biochem. 77 (2021) 577–587, https://doi.org/10.1007/s13105-021-00822-z.

[9] N. Zarkovic, Roles and Functions of ROS and RNS in Cellular Physiology and Pathology, Cells 9 (2020) 767, https://doi.org/10.3390/cells9030767.

[10] S. Cory, J.M. Adams, The Bcl2 family: regulators of the cellular life-or-death switch, Nat. Rev. Cancer 2 (2002) 647–656, https://doi.org/10.1038/nrc883.

[11] Y. Yue, H. Zhao, Y. Yue, Y. Zhang, W. Wei, Downregulation of Microrna-421 Relieves Cerebral Ischemia/Reperfusion Injuries: Involvement of Anti-apoptotic and Antioxidant Activities, NeuroMol. Med. 22 (2020) 411–419, https://doi.org/10.1007/s12017-020-08600-8.

[12] L. Zhuang, Y. Kong, S. Yang, F. Lu, Z. Gong, S. Zhan, M. Liu, Dynamic changes of inflammation and apoptosis in cerebral ischemia-reperfusion injury in mice

investigated by ferumoxytol-enhanced magnetic resonance imaging, Mol. Med. Rep. 23 (2021) 282, https://doi.org/10.3892/mmr.2021.11921.
[13] Y. Feinstein-Rotkopf, E. Arama, Can't live without them, can live with them: roles of caspases during vital cellular processes, Apoptosis 14 (2009) 980–995, https://doi.org/10.1007/s10495-009-0346-6.
[14] P.P. Wang, Y.J. Zhang, T. Xie, J. Sun, X.D. Wang, MiR-223 promotes cardiomyocyte apoptosis by inhibiting Foxo3a expression, Eur. Rev. Med. Pharmacol. Sci. 22 (2018) 6119–6126, https://doi.org/10.26355/eurrev_201809_15951.
[15] E.Y. Enioutina, E.R. Salis, K.M. Job, M.I. Gubarev, L.V. Krepkova, C.M. Sherwin, Herbal Medicines: challenges in the modern world. Part 5. status and current directions of complementary and alternative herbal medicine worldwide, Expert Rev. Clin. Pharmacol. 10 (2017) 327–338, https://doi.org/10.1080/17512433.2017.1268917.
[16] R.R. Green, N. Santoro, A.A. Allshouse, G. Neal-Perry, C. Derby, Prevalence of Complementary and Alternative Medicine and Herbal Remedy Use in Hispanic and Non-Hispanic White Women: Results from the Study of Women's Health Across the Nation, J. Altern. Complement. Med. 23 (2017) 805–811, https://doi.org/10.1089/acm.2017.0080.
[17] K. Gavaraskar, S. Dhulap, R.R. Hirwani, Therapeutic and cosmetic applications of Evodiamine and its derivatives–A patent review, Fitoterapia 106 (2015) 22–35, https://doi.org/10.1016/j.fitote.2015.07.019.
[18] W.Y. Huang, Y.Z. Cai, Y. Zhang, Natural phenolic compounds from medicinal herbs and dietary plants: potential use for cancer prevention, Nutr. Cancer 62 (2010) 1–20, https://doi.org/10.1080/01635580903191585.
[19] P. Lijnen, V. Petrov, R. Fagard, Induction of cardiac fibrosis by transforming growth factor-β1, Mol. Genet. Metab. 71 (2000) 418–435, https://doi.org/10.1006/mgme.2000.3032.
[20] A. Salimeh, M. Mohammadi, B. Rashidi, Preconditioning with diosgenin and treadmill exercise preserves the cardiac toxicity of isoproterenol in rats, J. Physiol. Biochem. 69 (2013) 255–265, https://doi.org/10.1007/s13105-012-0208-5.
[21] J. Wu, L. Wang, Y. Cui, F. Liu, J. Zhang, Allii Macrostemonis Bulbus: A Comprehensive Review of Ethnopharmacology, Phytochemistry and Pharmacology. Molecules 28 (2023) 2485, https://doi.org/10.3390/molecules28062485.
[22] H. Chen, W. Ou, G. Wang, N. Wang, L. Zhang, X. Yao, New Steroidal Glycosides Isolated as CD40L Inhibitors of Activated Platelets, Molecules 15 (2010) 4589–4598, https://doi.org/10.3390/molecules15074589.
[23] H. Feng, Z. Wang, C. Wang, X. Zhu, Z. Liu, H. Liu, M. Guo, Q. Hou, Z. Chu, Effect of Furostanol Saponins from Allium Macrostemon Bunge Bulbs on Platelet Aggregation Rate and PI3K/Akt Pathway in the Rat Model of Coronary Heart Disease, Evid. Based. Complement. Alternat. Med. 2019 (2019) 9107847, https://doi.org/10.1155/2019/9107847.
[24] Y.P. Lin, L.Y. Lin, H.Y. Yeh, C.H. Chuang, S.W. Tseng, Y.H. Yen, Antihyperlipidemic activity of Allium chinense bulbs, J. Food Drug. Anal. 24 (2016) 516–526, https://doi.org/10.1016/j.jfda.2016.01.010.
[25] W.C. Ou, H.F. Chen, Y. Zhong, B.R. Liu, S.M. Liu, K.J. Chen, Inhibition of platelet activation and aggregation by furostanol saponins isolated from the bulbs of Allium macrostemon Bunge, Am. J. Med. Sci. 344 (2012) 261–267, https://doi.org/10.1097/MAJ.0b013e31823ea9f0.
[26] R. Wang, L. Wang, M. Zhang, Y. Guo, J. Zhang, G. Ma, Five new spirosterol saponins from Allii Macrostemonis Bulbus, Chin. J. Nat. Med. 21 (2023) 226–232, https://doi.org/10.1016/S1875-5364(23)60423-6.
[27] J. Wu, L. Li, C. Liu, C. Li, Y. Cui, W. Ding, J. Zhang, L. Shi, Two New Compounds from Allii Macrostemonis Bulbus and Their In Vitro Antioxidant Activities, Molecules 28 (2023) 6176, https://doi.org/10.3390/molecules28176176.
[28] B.M. Al-Botaty, A. Elkhoely, A.A.E. Ahmed, Ethyl pyruvate attenuates isoproterenol-induced myocardial infarction in rats: Insight to TNF-α-mediated apoptotic and necroptotic signaling interplay, Int. Immunopharmacol. 103 (2022) 108495, https://doi.org/10.1016/j.intimp.2021.108495.
[29] P. Allawadhi, A. Khurana, N. Sayed, P. Kumari, C. Godugu, Isoproterenol-induced cardiac ischemia and fibrosis: Plant-based approaches for intervention, Phytother. Res. 32 (2018) 1908–1932, https://doi.org/10.1002/ptr.6152.
[30] R. Mu, S. Ye, R. Lin, Y. Li, X. Guo, L. An, Effects of Peroxiredoxin 6 and Its Mutants on the Isoproterenol Induced Myocardial Injury in H9C2 Cells and Rats, Oxid. Med. Cell. Longevity 2022 (2022) 2576310, https://doi.org/10.1155/2022/2576310.
[31] Z.W. Wong, P.V. Thanikachalam, S. Ramamurthy, Molecular understanding of the protective role of natural products on isoproterenol-induced myocardial infarction: A review, Biomed. Pharmacother. 94 (2017) 1145–1166, https://doi.org/10.1016/j.biopha.2017.08.009.
[32] K. Huynh, B.C. Bernardo, J.R. McMullen, R.H. Ritchie, Diabetic cardiomyopathy: mechanisms and new treatment strategies targeting antioxidant signaling pathways, Pharmacol. Ther. 142 (2014) 375–415, https://doi.org/10.1016/j.pharmthera.2014.01.003.
[33] M.A. Sussman, M. Völkers, K. Fischer, B. Bailey, C.T. Cottage, S. Din, N. Gude, D. Avitabile, R. Alvarez, B. Sundararaman, P. Quijada, M. Mason, M.H. Konstandin, A. Malhowski, Z. Cheng, M. Khan, M. McGregor, Myocardial AKT: the omnipresent nexus, Physiol. Rev. 91 (2011) 1023–1070, https://doi.org/10.1152/physrev.00024.2010.
[34] Q. Li, L. Shen, Z. Wang, H.P. Jiang, L.X. Liu, Tanshinone IIA protects against myocardial ischemia reperfusion injury by activating the PI3K/Akt/mTOR signaling pathway, Biomed. Pharmacother. 84 (2016) 106–114, https://doi.org/10.1016/j.biopha.2016.09.014.
[35] X. Tan, Y.F. Chen, S.Y. Zou, W.J. Wang, N.N. Zhang, Z.Y. Sun, W. Xian, X.R. Li, B. Tang, H.J. Wang, Q. Gao, P.F. Kang, ALDH2 attenuates ischemia and reperfusion injury through regulation of mitochondrial fusion and fission by PI3K/AKT/mTOR pathway in diabetic cardiomyopathy, Free Radical Biol. Med. 195 (2023) 219–230, https://doi.org/10.1016/j.freeradbiomed.2022.12.097.
[36] M. Zhang, X. Wang, M. Liu, D. Liu, J. Pan, J. Tian, T. Jin, Y. Xu, F. An, Inhibition of PHLPP1 ameliorates cardiac dysfunction via activation of the PI3K/Akt/mTOR signalling pathway in diabetic cardiomyopathy, J. Cell. Mol. Med. 24 (2020) 4612–4623, https://doi.org/10.1111/jcmm.15123.
[37] W.E. Nabofa, O.O. Alashe, O.T. Oyeyemi, A.F. Attah, A.A. Oyagbemi, T. O. Omobowale, A.A. Adedapo, A.R. Alada, Cardioprotective effects of curcumin-nisin based poly lactic acid nanoparticle on myocardial infarction in guinea pigs, Sci. Rep. 8 (2018) 16649, https://doi.org/10.1038/s41598-018-35145-5.
[38] Gbd, Diseases and Injuries Collaborators, 2020. Global burden of 369 diseases and injuries in 204 countries and territories, 1990–2019: a systematic analysis for the Global Burden of Disease Study 2019, Lancet 396 (2019) 1204–1222, https://doi.org/10.1016/S0140-6736(20)30925-9.
[39] C. Lin, Q. Sang, Z. Fu, S. Yang, M. Zhang, H. Zhang, Y. Wang, P. Hu, Deciphering mechanism of Zhishi-Xiebai-Guizhi Decoction against hypoxia/reoxygenation injury in cardiomyocytes by cell metabolomics: Regulation of oxidative stress and energy acquisition, J. Chromatogr. B: Anal. Technol. Biomed. Life Sci. 1216 (2023) 123603, https://doi.org/10.1016/j.jchromb.2023.123603.
[40] R.H. Christenson, H. Vaidya, Y. Landt, R.S. Bauer, S.F. Green, F.A. Apple, A. Jacob, G.R. Magneson, S. Nag, A.H. Wu, H.M. Azzazy, Standardization of creatine kinase-MB (CK-MB) mass assays: the use of recombinant CK-MB as a reference material, Clin. Chem. 45 (1999) 1414–1423, https://doi.org/10.1093/clinchem/45.9.1414.
[41] Z.Y. Liu, S.P. Hu, Q.R. Ji, H.B. Yang, D.H. Zhou, F.F. Wu, Sevoflurane pretreatment inhibits the myocardial apoptosis caused by hypoxia reoxygenation through AMPK pathway: An experimental study, Asian Pac. J. Trop. Med. 10 (2017) 148–151, https://doi.org/10.1016/j.apjtm.2017.01.006.
[42] E.H.M. Hassanein, A.S. Shalkami, M.M. Khalaf, W.R. Mohamed, R.A.M. Hemeida, The impact of Keap1/Nrf2, P(38)MAPK/NF-κB and Bax/Bcl2/caspase-3 signaling pathways in the protective effects of berberine against methotrexate-induced nephrotoxicity, Biomed. Pharmacother. 109 (2019) 47–56, https://doi.org/10.1016/j.biopha.2018.10.088.
[43] H.R. Li, X.M. Zheng, Y. Liu, J.H. Tian, J.J. Kou, J.Z. Shi, X.B. Pang, X.M. Xie, Y. Yan, L-Carnitine Alleviates the Myocardial Infarction and Left Ventricular Remodeling through Bax/Bcl-2 Signal Pathway, Cardiovasc. Ther. 2022 (2022) 9615674, https://doi.org/10.1155/2022/9615674.
[44] M. Neri, I. Riezzo, N. Pascale, C. Pomara, E. Turillazzi, Ischemia/Reperfusion Injury following Acute Myocardial Infarction: A Critical Issue for Clinicians and Forensic Pathologists, Mediators Inflammation 2017 (2017) 7018393, https://doi.org/10.1155/2017/7018393.
[45] H. Sies, Oxidative stress: a concept in redox biology and medicine, Redox. Biol. 4 (2015) 180–183, https://doi.org/10.1016/j.redox.2015.01.002.
[46] D.B. Zorov, M. Juhaszova, S.J. Sollott, Mitochondrial reactive oxygen species (ROS) and ROS-induced ROS release, Physiol. Rev. 94 (2014) 909–950, https://doi.org/10.1152/physrev.00026.2013.
[47] X. Wang, X. Lu, R. Zhu, K. Zhang, S. Li, Z. Chen, L. Li, Betulinic Acid Induces Apoptosis in Differentiated PC12 Cells Via ROS-Mediated Mitochondrial Pathway, Neurochem. Res. 42 (2017) 1130–1140, https://doi.org/10.1007/s11064-016-2147-y.
[48] L.Q. Yuan, C. Wang, D.F. Lu, X.D. Zhao, L.H. Tan, X. Chen, Induction of apoptosis and ferroptosis by a tumor suppressing magnetic field through ROS-mediated DNA damage, Aging (N. Y.) 12 (2020) 3662–3681, https://doi.org/10.18632/aging.102836.
[49] K. Maiese, Z.Z. Chong, Y.C. Shang, S. Wang, Targeting disease through novel pathways of apoptosis and autophagy, Expert Opin. Ther. Targets 16 (2012) 1203–1214, https://doi.org/10.1517/14728222.2012.719499.
[50] R.M. Wu, B. Jiang, H. Li, W.Z. Dang, W.L. Bao, H.D. Li, G. Ye, X. Shen, A network pharmacology approach to discover action mechanisms of Yangxinshi Tablet for improving energy metabolism in chronic ischemic heart failure, J. Ethnopharmacol. 246 (2020) 112227, https://doi.org/10.1016/j.jep.2019.112227.
[51] D.P. Brazil, B.A. Hemmings, Ten years of protein kinase B signalling: a hard Akt to follow, Trends. Biochem. Sci. 26 (2001) 657–664, https://doi.org/10.1016/s0968-0004(01)01958-2.
[52] B.D. Manning, A. Toker, AKT/PKB Signaling: Navigating the Network, Cell 169 (2017) 381–405, https://doi.org/10.1016/j.cell.2017.04.001.
[53] N. Very, A.S. Vercoutter-Edouart, T. Lefebvre, S. Hardivillé, I. El Yazidi-Belkoura, Cross-Dysregulation of O-GlcNAcylation and PI3K/AKT/mTOR Axis in Human Chronic Diseases, Front. Endocrinol. 9 (2018) 602, https://doi.org/10.3389/fendo.2018.00602.
[54] X. Shang, K. Lin, R. Yu, P. Zhu, Y. Zhang, L. Wang, J. Xu, K. Chen, Resveratrol Protects the Myocardium in Sepsis by Activating the Phosphatidylinositol 3-Kinases (PI3K)/AKT/Mammalian Target of Rapamycin (mTOR) Pathway and Inhibiting the Nuclear Factor-κB (NF-κB) Signaling Pathway, Med. Sci. Monit. 25 (2019) 9290–9298, https://doi.org/10.12659/MSM.918369.
[55] M. Wan, K. Yin, J. Yuan, S. Ma, Q. Xu, D. Li, H. Gao, X. Gou, YQFM alleviated cardiac hypertrophy by apoptosis inhibition and autophagy regulation via PI3K/AKT/mTOR pathway, J. Ethnopharmacol. 285 (2022) 114835, https://doi.org/10.1016/j.jep.2021.114835.
[56] Z. Jia, L. Lin, S. Huang, Z. Zhu, W. Huang, Z. Huang, Inhibition of autophagy by berberine enhances the survival of H9C2 myocytes following hypoxia, Mol. Med. Rep. 16 (2017) 1677–1684, https://doi.org/10.3892/mmr.2017.6770.
[57] J.K. Jin, E.A. Blackwood, K. Azizi, D.J. Thuerauf, A.G. Fahem, C. Hofmann, R. J. Kaufman, S. Doroudgar, C.C. Glembotski, ATF6 Decreases Myocardial Ischemia/Reperfusion Damage and Links ER Stress and Oxidative Stress Signaling Pathways

in the Heart, Circ. Res. 120 (2017) 862–875, https://doi.org/10.1161/CIRCRESAHA.116.310266.
[58] K. Nishida, O. Yamaguchi, K. Otsu, Crosstalk between autophagy and apoptosis in heart disease, Circ. Res. 103 (2008) 343–351, https://doi.org/10.1161/CIRCRESAHA.108.175448.
[59] C.D. Ochoa, R.F. Wu, L.S. Terada, ROS signaling and ER stress in cardiovascular disease, Mol. Aspects Med. 63 (2018) 18–29, https://doi.org/10.1016/j.mam.2018.03.002.
[60] O.E. Osadchii, Cardiac hypertrophy induced by sustained beta-adrenoreceptor activation: pathophysiological aspects, Heart Failure Rev. 12 (2007) 66–86, https://doi.org/10.1007/s10741-007-9007-4.